ACS Chemical Neuroscience

Review

pubs.acs.org/chemneuro

Modulation of Amyloid β-Protein (Aβ) Assembly by Homologous C-Terminal Fragments as a Strategy for Inhibiting Aβ Toxicity

Huiyuan Li,[†] Farid Rahimi,[‡] and Gal Bitan*[,§]

[†]West Virginia University, Morgantown, West Virginia 26506, United States

[‡]Biomedical Science and Biochemistry, Research School of Biology, The Australian National University, Acton, ACT 2601, Australia

[§]Department of Neurology, David Geffen School of Medicine, Brain Research Institute, and Molecular Biology Institute, University of California at Los Angeles, Neuroscience Research Building 1, Room 451 635 Charles E. Young Drive South, Los Angeles, California 90095-7334, United States

ABSTRACT: Self-assembly of amyloid β-protein (Aβ) into neurotoxic oligomers and fibrillar aggregates is a key process thought to be the proximal event leading to development of Alzheimer's disease (AD). Therefore, numerous attempts have been made to develop reagents that disrupt this process and prevent the formation of the toxic oligomers and aggregates. An attractive strategy for developing such reagents is to use peptides derived from Aβ based on the assumption that such peptides would bind to full-length Aβ, interfere with binding of additional full-length molecules, and thereby prevent formation of the toxic species. Guided by this rationale, most of the studies in the last two decades have focused on preventing formation of the core cross-β structure of Aβ amyloid fibrils using β-sheet-breaker peptides derived from the central hydrophobic cluster of Aβ. Though this approach is effective in inhibiting fibril formation, it is generally inefficient in preventing Aβ oligomerization. An alternative approach is to use peptides derived from the C-terminus of Aβ, which mediates both oligomerization and fibrillogenesis. This approach has been explored by several groups, including our own, and led to the discovery of several lead peptides with moderate to high inhibitory activity. Interestingly, the mechanisms of these inhibitory effects have been found to be diverse, and only in a small percentage of cases involved interference with β-sheet formation. Here, we review the strategy of using C-terminal fragments of Aβ as modulators of Aβ assembly and discuss the relevant challenges, therapeutic potential, and mechanisms of action of such fragments.

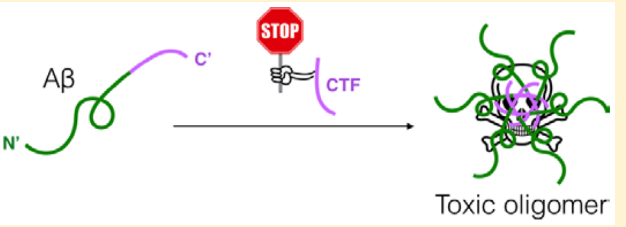

KEYWORDS: *Alzheimer's disease, amyloid, peptide, aggregation, oligomerization, toxicity*

Abnormal folding and self-assembly of proteins into toxic oligomers and amyloid fibrils is believed to be the underlying cause of over 50 severe diseases and pathologic conditions jointly called *proteinopathies*. Classic examples are Alzheimer's,[5] Parkinson's,[6] and Huntington's[7] diseases. The number of recognized proteinopathies has been increasing gradually as additional abnormal protein deposits have been found in multiple other diseases, such as different variants of amyotrophic lateral sclerosis, frontotemporal dementia,[8] mental disorders,[9] and preeclampsia.[10]

Research on the molecular events linking protein misfolding and aggregation to disease has been led by studies of amyloid β-protein (Aβ) in Alzheimer's disease (AD). Substantial genetic, biological, and biochemical evidence suggests that self-association of Aβ monomers into neurotoxic oligomers initiates a pathologic cascade that leads to AD development. Therefore, tremendous effort has been dedicated to understanding the process of Aβ self-assembly and development of strategies to interfere with this process.

One of the earliest approaches to interrupting formation of toxic Aβ assemblies has been using homologous peptides derived from different regions of the Aβ sequence itself. This strategy is based on self-recognition by these peptides and the idea that an Aβ fragment would bind to a complementary sequence in the full-length protein and interfere with subsequent binding of additional Aβ molecules. The first attempts to design peptides based on these ideas used sequences derived from the central hydrophobic cluster (CHC, residues 17−21) of Aβ, and to date, this is still the most popular approach. Aβ CHC was found early on to be crucial for formation of the core cross-β structure of Aβ amyloid fibrils.[11] Peptides derived from this region generally were designed as β-sheet breakers by incorporating either N-methylated residues or residues that would be incompatible with a β-strand, such as proline, both consequently preventing binding by an oncoming molecule and increasing the metabolic stability of the peptide (for a detailed discussion of this approach, see ref 12).

An important gradual realization over the last two decades has been that the amyloid fibrils found in the brain of patients with AD are not the cause of the disease, as originally posited by the *amyloid cascade hypothesis*.[13] Rather, evidence from

Received: May 29, 2016
Accepted: June 20, 2016

DOI: 10.1021/acschemneuro.6b00154
ACS Chem. Neurosci. XXXX, XXX, XXX−XXX

studies in cell culture, animal models, and patients with AD have all supported the view that water-soluble Aβ oligomers are the actual culprits.[14,15] Because the oligomers are metastable species that exist in dynamically changing mixtures, studying their structures in detail and conceiving of ways to interfere with their formation have been substantial challenges.[16] Nonetheless, this shift in the understanding of the underlying mechanisms by which Aβ affects synapses and neurons in AD suggested that β-sheet-breaker peptides might not be effective enough if they disrupt only the β-sheet structure of Aβ fibrils and not those of Aβ oligomers.

An alternative approach suggested that peptides derived from Aβ C-terminus might be able to interfere with Aβ oligomerization because several lines of evidence suggested that the stretch of mainly hydrophobic amino acids in the C-terminus, particularly in the long form of Aβ, Aβ42, likely formed the core of the oligomers.[17−21] This stretch comprises 14 C-terminal nonpolar residues, Aβ(29−42) (Figure 1).

^{1}DAEFRHDSGY^{10}EVHHQKLVFF^{20}AEDVGSNKGA^{30}IIGLMVGGVV^{40}IA

Figure 1. Amino acid sequence of Aβ42. Color code: Brown = nonpolar, purple = polar, blue = negatively charged, and magenta = positively charged. The CHC and C-terminal regions are underlined.

Based on this evidence, we and others have hypothesized that peptides derived from the C-terminus of Aβ42 (C-terminal fragments, CTFs), when mixed with full-length Aβ42, might partition into the oligomer core and disrupt it. We discuss below the challenges, findings, and advantages of this strategy and its potential for yielding effective drug candidates for AD.

CHALLENGES IN SYNTHESIZING Aβ C-TERMINAL FRAGMENTS

Synthesis and purification of peptides containing mainly hydrophobic amino acids are challenging because such peptides tend to aggregate and have low solubility in typical solvents, such as *N*,*N*-dimethylformamide or *N*-methylpyrrolidone, used for solid-phase peptide synthesis.[22−25] Because Aβ CTFs are predominantly made of hydrophobic amino acids, synthesizing fragments above a certain length (7−8 amino acids) becomes difficult. In addition, the tendency of CTFs to self-assemble into β-sheet-rich amyloid fibrils increases their aggregation propensity, making their synthesis and purification even more difficult.[24,25]

To study the CTFs as inhibitors of Aβ42 aggregation and Aβ42-induced neurotoxicity, our group synthesized a series of Aβ42 CTFs [Aβ(*x*−42), *x* = 28−39] using 9-fluorenylmethoxycarbonyl chemistry. We applied several strategies to synthesizing these difficult sequences.[26] First, it was important to use resins of relatively low loading capacity to minimize on-resin peptide aggregation. Though in initial experiments we synthesized CTFs successfully using 200−400-mesh 0.7 mmol/g Wang resin from Bachem and 200−400-mesh 0.4−0.6 mmol/g Wang resin from Novabiochem, later we found resins of low loading capacities, such as 100−200-mesh Wang resin from Novabiochem with <0.5 mmol/g substitution level, to be advantageous. We used these to successfully synthesize short CTFs, Aβ(39−42) through Aβ(33−42). The longer CTFs were synthesized using a 100−200-mesh TGA resin with 0.2−0.3 mmol/g substitution level from Novabiochem. For synthesis of CTFs with C-terminal amide groups, 100−200-mesh, 0.4−0.8 mmol/g peptide−amide linker resin worked well. Second, we used microwave-assisted peptide synthesis to improve peptide yields.[2,27] The microwave energy can disrupt aggregation through dipole rotation of the polar peptide backbone[28] and potentially improve coupling efficiency. Third, we extended durations of coupling and deprotection cycles beyond the manufacturer-recommended times: from 30 and 10 min to 60 and 30 min, respectively. The extended coupling and deprotection durations improved coupling efficiency as reported previously.[29]

Isolation of CTFs from crude cleavage mixtures was relatively straightforward for Aβ(39−42) through Aβ(35−42) and Aβ(28−42) but was difficult for Aβ(34−42) through Aβ(29−42). For short CTFs and Aβ(28−42), after cleavage from the resin using a trifluoroacetic acid (TFA)-based cocktail,[26] the peptide was precipitated out of the solution by adding cold diethyl ether. Then the crude peptide was purified using high-performance liquid chromatography (HPLC) on a C4 column. In contrast, this purification protocol failed for Aβ(34−42) through Aβ(29−42) because upon dilution of the concentrated cleavage mixture in ice-cold diethyl ether, these peptides remained soluble and thus did not precipitate. Attempts to load the crude cleavage mixture directly onto the HPLC column or diluting the TFA solution in mixtures of H_2O/acetonitrile/hexafluoroisopropanol or tetrafluoroethanol did not yield satisfactory results. Either yields were low or side products were found following HPLC purification, and only negligible amounts of the desired products were obtained. To overcome these problems, we modified the purification protocol and found that long CTFs could be isolated by water precipitation out of the TFA solution yielding high purity and alleviating the necessity of subsequent HPLC purification.[26] By this method, the long CTFs were obtained at ∼20% total yields. In later experiments, we found that by slowly pipetting droplets of concentrated Aβ(31−42) derivatives' cleavage solution (total ∼1−2 mL) into cold diethyl ether and then further cooling the mixture in a −20 °C freezer overnight, we could precipitate out the peptides from diethyl ether well. Then the crude peptides could be successfully purified using HPLC using a C4 column.[26]

PHYSICAL AND CHEMICAL CHARACTERISTICS OF C-TERMINAL FRAGMENTS

Evaluation of the efficacy of the CTF series described above as inhibitors of Aβ42-induced toxicity showed that all of them except the longest fragment, Aβ(28−42), inhibited Aβ42-induced toxicity significantly (Table 1).[30] Aβ(28−42) not only did not inhibit Aβ42 toxicity but actually displayed high toxicity itself. Of all the CTFs, Aβ(28−42) is the only peptide that carries a net positive charge, suggesting that its charge might have contributed to its observed toxicity, possibly by facilitating its binding to negatively charged phospholipid membrane bilayers.

Aβ(28−42) structure has been studied in aqueous environments as a fusion protein to three different C-terminally truncated forms of ribonuclease HII (*Tk*-RNase HII) from *Thermococcus kodakarensis*, a thermophilic archaea.[31] Unlike Aβ42, *Tk*-RNase HII is relatively stable and its C-terminus has limited interaction with other regions of the protein.[31] Circular dichroism (CD) spectroscopy and thermal denaturation experiments showed that the guest Aβ(28−42) did not affect the overall structure of the host protein. However, crystal structures of the *Tk*-RNase HII(1−197)−Aβ(28−42) fusion showed that Aβ(28−42) formed β-sheets.[31] This result is in

DOI: 10.1021/acschemneuro.6b00154
ACS Chem. Neurosci. XXXX, XXX, XXX−XXX

Table 1. Inhibition of Aβ42-Induced Toxicity by CTFs and Control Peptides

peptide	sequence	cell viability[a] (%)
Aβ(39−42)	VVIA	89 ± 5***
Aβ(38−42)	GVVIA	83 ± 3***
Aβ(37−42)	GGVVIA	73 ± 2***
Aβ(36−42)	VGGVVIA	80 ± 3***
Aβ(35−42)	MVGGVVIA	82 ± 4***
Aβ(34−42)	LMVGGVVIA	76 ± 3***
Aβ(33−42)	GLMVGGVVIA	81 ± 3***
Aβ(32−42)	IGLMVGGVVIA	79 ± 2***
Aβ(31−42)	IIGLMVGGVVIA	105 ± 5***
Aβ(30−42)	AIIGLMVGGVVIA	97 ± 4***
Aβ(29−42)	GAIIGLMVGGVVIA	72 ± 3**
Aβ(28−42)	KGAIIGLMVGGVVIA	
Aβ(34−40)	LMVGGVV	66 ± 2
Aβ(30−40)	AIIGLMVGGV	98 ± 7***

[a]Cell viability (mean ± SEM) was calculated from at least three independent experiments with 6 replicates per data point ($n \geq 18$). Statistical significance was calculated compared with Aβ42 alone using *t*-test. ***$p < 0.001$. **$p < 0.01$.

agreement with our studies using nonfused Aβ(28−42) and Aβ(29−42).[3] Aβ(28−42) fusion also caused aggregation of the host protein determined by the ThT assay,[31] demonstrating its high amyloidogenic propensity. However, because several shorter CTFs also formed β-sheet-rich amyloid fibrils, this property likely was not directly responsible for the high toxicity of Aβ(28−42).

Among all the other CTFs, Aβ(31−42) was the strongest inhibitor, followed by Aβ(30−42) and, surprisingly, Aβ(39−42). Thus, toxicity inhibition did not correlate with peptide length and had a complex relationship with peptide sequence. To decipher this relationship, we asked how each sequence might relate to the biophysical properties of each peptide and what structural/biophysical features contributed to inhibition of Aβ42-induced toxicity. To answer these questions, we studied the biophysical properties of Aβ42 CTFs. We also compared them with two Aβ40 CTFs, which provided further insight into the structure−activity relationship.[3]

Solubility studies (see ref 3 for details of sample preparation) showed that CTFs up to 10 amino acids long were soluble between ∼100 and ∼200 μM. Longer peptides were soluble between ∼10 and ∼80 μM, except for the longest CTF, Aβ(28−42), which had the lowest solubility, ∼ 1 μM, despite having an extra charge. The two Aβ40 CTFs, Aβ(34−40) and Aβ(30−40), had higher solubility than any of the Aβ42 CTFs. This observation accorded with the hypothesis that the two C-terminal residues, Ile41 and Ala42, stabilize aggregation-prone conformations in Aβ42.[17,20]

The same samples used for the solubility studies were characterized further for time-dependent particle growth, conformational change, and morphology using dynamic light scattering (DLS), CD spectroscopy, and electron microscopy (EM), respectively. Particle growth was observed for Aβ(*x*−42) with x = 29, 30, 31, and 33, and for Aβ(30−40), but not for other CTFs, which apparently did not aggregate. The change in hydrodynamic radius (R_H) of these CTFs over 96 h is shown in Figure 2A, and the average particle growth rates (dR_{H2}/dt) are given in Figure 2B. The general trend among the four Aβ42 CTFs was faster aggregation with longer sequence, but the correlation between length and aggregation kinetics was not linear. Aβ(29−42) and Aβ(30−42) aggregated substantially faster than Aβ(31−42) and Aβ(33−42) even though they were measured at substantially lower concentrations. Aβ(30−40) aggregated more slowly than the four Aβ42 CTFs despite similar length, demonstrating the strong contribution of the Ile41−Ala42 dipeptide to promoting aggregation. In fact, Aβ(30−40) and Aβ(32−42) share the same amino acid composition and 82% sequence identity (Figure 3), yet as demonstrated in the experiments described below, their biophysical, biochemical, and inhibitory characteristics were distinct.

```
Aβ(30-40)  AIIGLMVGGVV
Aβ(32-42)    IGLMVGGVVIA
```

Figure 3. Sequence alignment of Aβ(30−40) and Aβ(32−42).

In parallel to the DLS measurements, CD spectra of each peptide were recorded over 96 h. The initial spectra of all

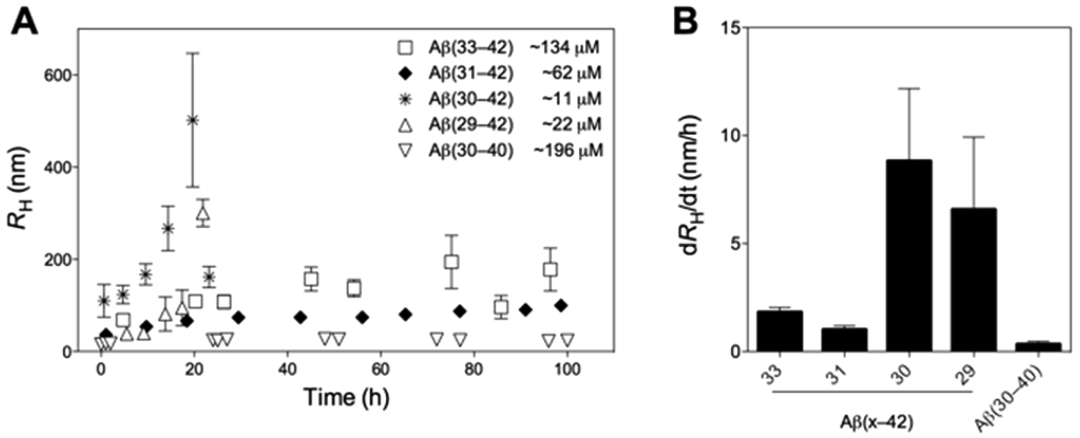

Figure 2. Particle growth rate. (A) Time course of average R_H was calculated from whole particle size distributions in solutions of Aβ(29−42), Aβ(30−42), Aβ(31−42), Aβ(33−42), or Aβ(30−40) at indicated concentrations. Each data point represents mean ± SEM calculated from the average R_H of eight consecutive DLS measurements during 45−60 min. Aggregation of Aβ(29−42) and Aβ(30−42) was followed until the upper limit of detection was reached. (B) Average aggregation rates of Aβ(29−42), Aβ(30−42), Aβ(31−42), Aβ(33−42), and Aβ(30−40). The data represent mean ± SEM of three independent experiments. Reproduced from ref 3. Copyright 2010 American Chemical Society.

DOI: 10.1021/acschemneuro.6b00154
ACS Chem. Neurosci. XXXX, XXX, XXX−XXX

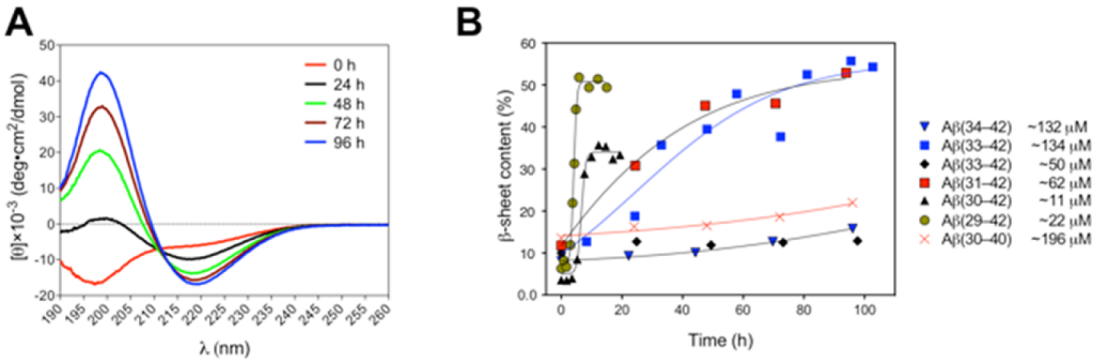

Figure 4. Time-dependent conformational changes during CTF aggregation. (A) Representative CD spectra of 62 μM Aβ(31−42) recorded in 24-h time intervals. (B) Representative time course of β-sheet formation shown for Aβ(29−42), Aβ(30−42), Aβ(31−42), Aβ(33−42), Aβ(34−42), and Aβ(30−40) at the indicated concentrations. Reproduced from ref 3. Copyright 2010 American Chemical Society.

peptides showed a high proportion of unordered structure. The spectra of Aβ(32−42), Aβ(35−42) through Aβ(39−42), and Aβ(34−40) did not change during the experiment. The other peptides showed a time-dependent spectral change indicating transformation from unordered conformation to a β-sheet-rich structure. Figure 4A shows characteristic CD spectra of ∼60 μM Aβ(31−42) as an example. An isodichroic point was observed at 212 nm, suggesting a one-step transition from unstructured to β-sheet-rich conformation. As shown in Figure 4B, the longer peptides showed faster β-sheet conversion. Aβ(29−42) and Aβ(30−42) converted to β-sheet structures within several hours, whereas Aβ(34−42) and Aβ(30−40) showed a small increase in β-sheet content during the time of experiment. Aβ(33−42) did not show conformational conversion at ∼50 μM, but at ∼130 μM, it converted to β-sheet at a rate similar to that of Aβ(31−42) at ∼60 μM. Consistent with the DLS results, Aβ(32−42) behaved as an outlier. At ∼55 μM, Aβ(32−42) showed no conformational changes up to 96 h.

To determine the morphologies of peptide aggregates, aliquots of each peptide solution were examined by EM directly after dissolution and following incubation for 7 days. Electron micrographs of Aβ(35−42) through Aβ(39−42) and Aβ(34−40) showed nonfibrillar aggregates. Aβ(34−42) and longer Aβ42 CTFs, except Aβ(32−42), were found to form fibrils that displayed substantial morphological variability.[3]

Through physical and chemical characterization of CTFs in DLS, CD, and EM experiments, we found that most Aβ42 CTFs longer than eight residues readily formed β-sheet-rich fibrils, whereas the shorter CTFs did not. The two Aβ40 CTFs were substantially less prone to aggregation than their Aβ42 CTF counterparts. Aβ(32−42) behaved anomalously for reasons that are yet unclear. In particular, the lack of observed aggregation and conformational change were surprising in view of the fact that Aβ(33−42) did aggregate. Based on length only, Aβ(32−42) would have been expected to aggregate at an intermediate rate between Aβ(33−42) and Aβ(31−42), yet no aggregation was observed.

The structure of Aβ(34−42) fibrils was studied by Lansbury et al., who measured the intramolecular ^{13}C−^{13}C distances and ^{13}C chemical shifts using solid-state ^{13}C NMR and individual amide absorption frequencies by isotope-edited infrared spectroscopy. An antiparallel β-sheet structure was observed.[32] This arrangement was found also for other short sequences derived from Aβ, whereas full-length Aβ40 and Aβ42 formed parallel β-sheets.[33] Based on these data, it is likely that the shorter CTFs used in our studies form antiparallel β-sheets whereas the longer ones may prefer the parallel arrangement, but experimental evidence is unavailable.

Aβ(32−37) was synthesized by Pratim Bose et al. with N-methylation at various positions.[1,34] They hypothesized that N-methylated peptides could inhibit Aβ self-assembly because these peptides tend to adopt an extended β-strand conformation and disrupt the self-assembly process. The Aβ(32−37) analogues contained zero, two, three, or five N-methylation sites (Figure 5). Examination of the peptides by CD spectroscopy at 100 μM did not show any spectral changes for 5 h, suggesting that the peptides did not aggregate during this time[1] similarly to the shorter peptides in the CTF series described above. The dimethylated and pentamethylated peptides were soluble in aqueous buffers at concentrations

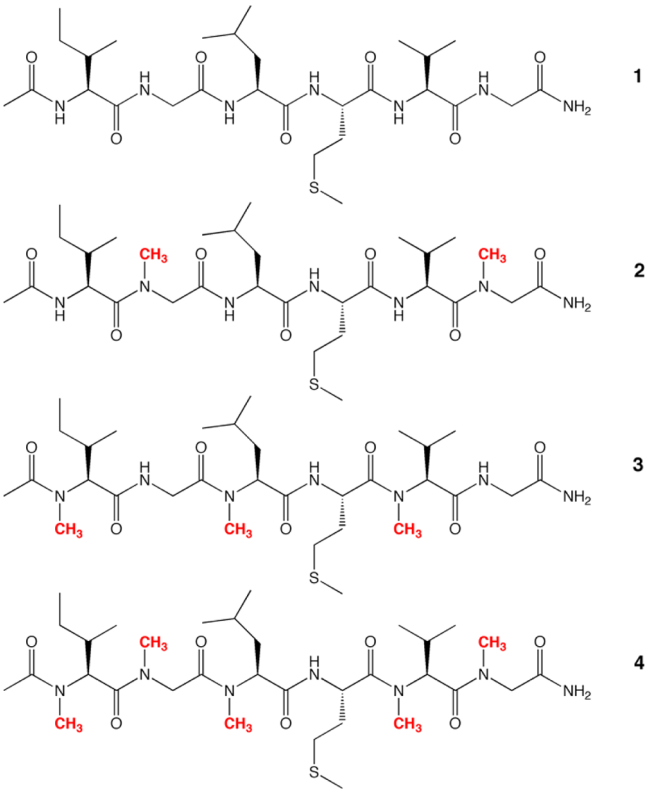

Figure 5. Structures of the N-Methylated Peptides 1−4. Reproduced from ref 1. Copyright 2009 American Chemical Society.

DOI: 10.1021/acschemneuro.6b00154
ACS Chem. Neurosci. XXXX, XXX, XXX−XXX

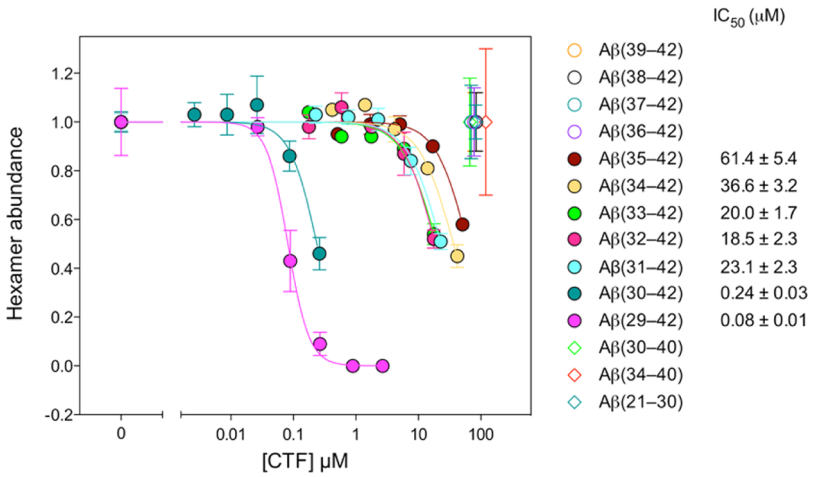

Figure 6. Inhibition of Aβ42 hexamer formation. Aβ42 was cross-linked in the absence or presence of increasing concentrations of each CTF and analyzed by SDS−PAGE and silver staining. Aβ(21−30) was used as a negative control. The amount of Aβ42 hexamer was determined densitometrically and normalized to the protein content in the entire lane. IC_{50} values are the CTF concentrations required for 50% inhibition of Aβ42 hexamer formation. Reproduced from ref 4. Copyright 2010 American Chemical Society.

exceeding 2.5 mM,[34] a typical characteristic of N-methylated amyloidogenic peptides.

Recently, Jain and co-workers have used Aβ(32−37)-NH_2 as a starting point for structure−activity relationship (SAR) studies in which each of the six residues was replaced by various native or non-native amino acids.[35] Unlike the studies by Pratim Bose et al., these analogues had a free N-terminus and no N-methylated peptide bonds. Though the solubility of the peptides was not discussed explicitly, the fact that they were dissolved first in DMSO and then diluted into PBS suggests that they had relatively low solubility in aqueous solutions.

Sequences derived from the region Aβ(31−34) or Aβ(31−35), including propionyl-IIGL-NH_2 (Pr-$IIGL_a$) and RIIGL-NH_2 ($RIIGL_a$) were studied by the Penke group.[36−39] Aβ(31−35)-NH_2 and $RIIGL_a$ did not aggregate after 6 days. In contrast, Pr-$IIGL_a$ strongly tended to aggregate and formed 2−3 μm long and 10−40 nm wide fibrils observed by EM.[36]

In conclusion, studies of unmodified CTFs from different groups have found that CTFs, especially long CTFs, tended to aggregate into β-sheet-rich fibrils. However, comparison among these different peptides showed that their aggregation propensity itself did not correlate with their ability to inhibit aggregation of full-length Aβ42.

BIOCHEMICAL AND BIOPHYSICAL CHARACTERISTICS OF C-TERMINAL FRAGMENT INTERACTIONS WITH FULL-LENGTH Aβ

Our group used photoinduced cross-linking of unmodified proteins (PICUP)[40,41] and DLS to study Aβ42 assembly in the absence or presence of CTFs. Previously, by PICUP,[42] the oligomer size distribution of Aβ42 was found to contain abundant pentamers and hexamers, which were termed "paranuclei".[17] The abundance of paranuclei, particularly the hexamers, was found to be a sensitive probe for testing inhibition of Aβ42 oligomerization.[41] Aβ42 was filtered through a 10 000 Da molecular-weight cutoff filter[43] to yield a ~30 μM solution containing only monomers and small oligomers, then mixed with increasing concentrations of each CTF, and subjected to PICUP. The cross-linked mixtures were analyzed by SDS−PAGE and band intensity was quantified densitometrically. Aβ(36−42) and shorter Aβ42 CTFs at concentrations >100 μM, as well as Aβ40 CTFs, did not inhibit Aβ42 hexamer formation. In contrast, Aβ(35−42) and longer CTFs decreased Aβ42 hexamer abundance dose-dependently (Figure 6). The inhibitory activity increased with peptide length from Aβ(35−42) through Aβ(33−42), whereas additional elongation to Aβ(32−42) and Aβ(31−42) had little effect on activity. Remarkably, further elongation to Aβ(30−42) and Aβ(29−42) increased the inhibitory activity by ~2 orders of magnitude, yielding nanomolar IC_{50} values.[4]

To complement the PICUP experiments, DLS was used to study Aβ42 particle growth in the absence or presence of CTFs. Of the 12 Aβ42 CTFs, six were selected for DLS characterization of their interactions with full-length Aβ42. In the absence of CTFs immediately after preparation, Aβ42 comprised predominantly two populations of particles: particles with a hydrodynamic radius R_{H1} = 8−12 nm, which remained largely unchanged during the measurements, and particles with an R_{H2} = 20−60 nm, which were observed in some measurements and tended to fluctuate substantially (Figure 7, bottom panel). We named these oligomer populations P_1 and P_2, respectively. Substantial differences in the P_2 growth rate, dR_{H2}/dt, were observed in the presence of different CTFs (Figure 7). The strongest toxicity inhibitor, Aβ(31−42), decreased dR_{H2}/dt substantially by 60% ± 13% relative to that of Aβ42 alone. Aβ(39−42) had a weaker effect on dR_{H2}/dt, decreasing the rate by 35% ± 28%. Other CTFs had little or no effect.[4] Interestingly, on day 1, smaller R_H values were observed in the presence of Aβ(39−42) (R_{H1} = 6 ± 3 nm, and R_{H2} = 30 ± 10 nm) relative to those with other CTFs. Similarly, in the presence of Aβ(30−40), P_1 particles had an R_{H1} of 6 ± 3 nm on day 1, though P_2 particles were larger than in the presence of other CTFs. Because both peptides were among the strongest inhibitors of Aβ42-induced toxicity, these data suggested a correlation between inhibition of toxicity and the smaller size of oligomers corresponding to P_1 particles. Taken together, the biochemical and biophysical studies of CTFs interactions with Aβ showed that CTFs longer than eight residues interrupted Aβ42 oligomerization, and the order of activity of the CTFs in inhibiting hexamer formation roughly followed CTF length, that is, longer CTFs were more efficacious in inhibiting hexamer formation. DLS measurements showed that CTFs

DOI: 10.1021/acschemneuro.6b00154
ACS Chem. Neurosci. XXXX, XXX, XXX−XXX

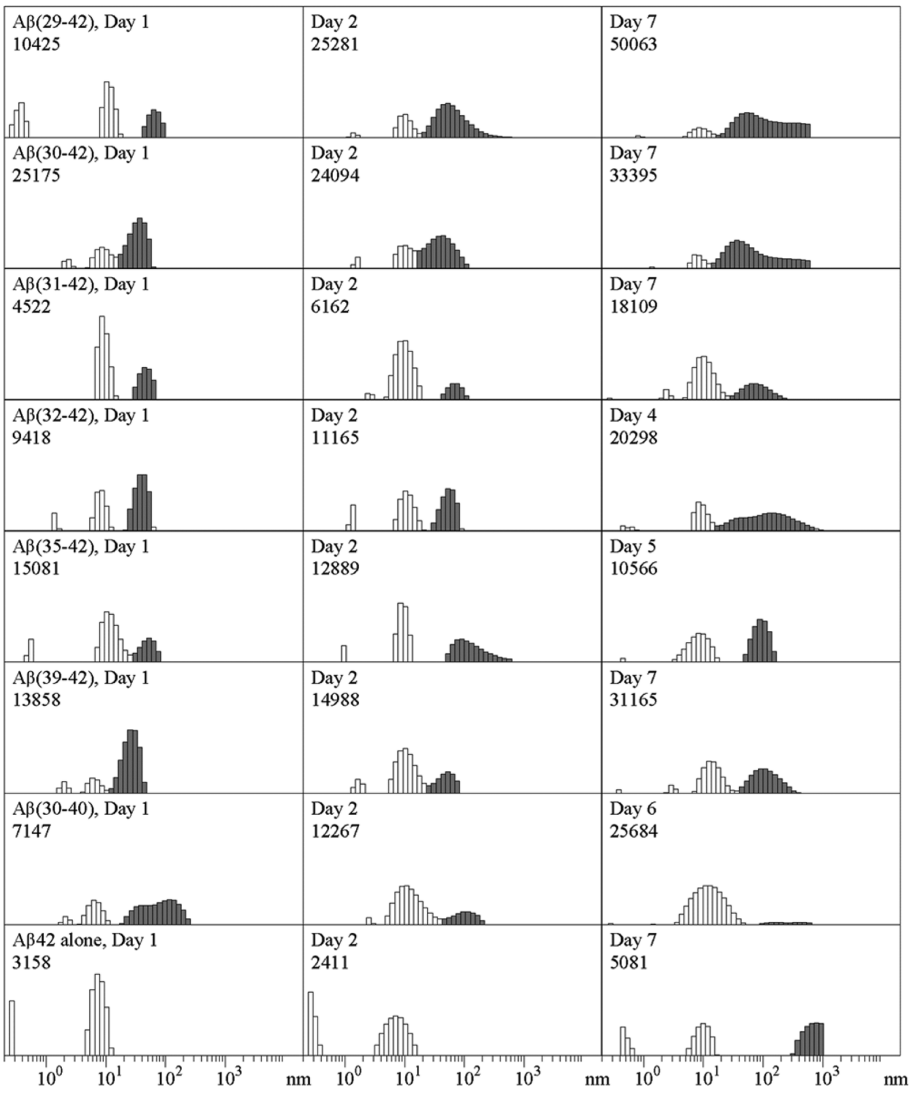

Figure 7. CTF effects on Aβ42 particle size distribution. Representative distribution of Aβ42 in the absence or presence of CTFs immediately after preparation (left), on the next day (center), and after 4−7 days (right). White bars represent data from P_1 particles. Gray bars represent data for P_2 or larger particles (in the case of Aβ42 alone). The numbers in the upper left corner correspond to the total scattering intensity measured in each sample. Reproduced from ref 4. Copyright 2010 American Chemical Society.

could stabilize two oligomer populations, P_1 and P_2. Strong toxicity inhibitors had a tendency to reduce the size of P_1 and attenuate the growth rate of P_2.[4]

Pratim Bose et al. assessed the effects of the N-methylated derivatives of Aβ(32−37) on Aβ40 and Aβ42 aggregation, initially using CD spectroscopy.[1] Aβ40 or Aβ42 (20 μM) was mixed with 100 μM of each of the four peptides in 10 mM sodium phosphate, and CD spectroscopy was used to monitor β-sheet formation. Peptide CD spectra were subtracted from the corresponding spectra of inhibitor-treated Aβ preparations. In these experiments, unordered structures changed to β-sheet structures (loss of minimum at ∼200 nm and appearance of a broad minimum at ∼217 nm) after 2 h for Aβ42 and after 4 h for Aβ40. The four peptides affected the initial β-sheet formation in both Aβ40 and Aβ42 but were more effective against Aβ40 than against Aβ42. The nonmethylated peptide 1 and the dimehtylated or trimethylated peptides 2 or 3 delayed β-sheet formation in Aβ40 or Aβ42 by 2−3 and 1 h, respectively. The pentamethylated peptide 4 completely prevented β-sheet formation in Aβ40 during the duration of the experiments and delayed β-sheet formation in Aβ42 by 2 h.

Congo-red (CR)-binding assay also was used to assess the effect of peptides 1−4 on formation of Aβ fibrils. In agreement with the CD results, peptide 4 reduced formation of CR-positive amyloid fibrils of Aβ40 or Aβ42, whereas peptides 1−3 were less effective.

The Aβ(32−37)-NH_2 analogue series examined by Jain et al. contained 42 peptides that were screened initially for their ability to inhibit Aβ40-induced toxicity in the 3-(4,5-dimethylthiazol-2-yl)-2,5-diphenyltetrazolium bromide (MTT) reduction assay in nondifferentiated rat pheochromocytoma PC-12 cells. Aβ(32−37)-NH_2 itself had the strongest inhibitory activity, followed by peptides containing the substitutions Ile32 → Val and Gly37 → Nle. Curiously, although the peptides were tested at Aβ40/fragment concentration ratios 1:1, 1:5, and 1:10, no dose−response relationship was apparent.[35]

Subsequent examination of the effect of Aβ(32−37)-NH_2 on Aβ fibrillogenesis showed that the fragment attenuated ThT fluorescence increase in both Aβ40 and Aβ42, delayed the

DOI: 10.1021/acschemneuro.6b00154
ACS Chem. Neurosci. XXXX, XXX, XXX−XXX

typical conformational transition measured by CD spectroscopy, and prevented fibril formation in TEM and scanning transmission electron microscopy measurements.[35]

In a study by the Penke group, Pr-IIGL$_a$ and RIIGL$_a$ were tested for inhibition of Aβ aggregation using CR binding and EM. Both analogues attenuated Aβ42 fibril formation at a 5-fold molar excess. RIIGL$_a$ was a stronger inhibitor than Pr-IIGL$_a$.[36] The studies described above suggested that most of the CTFs examined, modified or unmodified, interfered with full-length Aβ assembly as predicted. However, the mechanism of the interference appeared to be more complex than originally expected and different CTFs appeared to act at different stages of the assembly process, as discussed below.

CHARACTERIZATION OF THE INHIBITORY EFFECT OF C-TERMINAL FRAGMENTS ON Aβ-INDUCED TOXICITY AND THEIR MECHANISM OF ACTION

The efficacy of our Aβ42 CTFs as inhibitors of Aβ42-induced neurotoxicity[30] was evaluated initially using the MTT assay[44,45] in differentiated PC-12 cells[46,47] using 5 μM Aβ42 and 10-fold excess of each peptide. Aβ42 alone caused a robust (~40%) reduction in cell viability. All CTFs except Aβ(28−42) inhibited Aβ42-induced toxicity significantly. Of the 12 CTFs tested, Aβ(30−42), Aβ(31−42), and Aβ(39−42) were the strongest inhibitors[30] (Table 1). In addition, of the Aβ40 CTFs, Aβ(30−40) inhibited Aβ42-induced toxicity strongly, similar to Aβ(39−42) and Aβ(31−42), whereas Aβ(34−40) was inactive.[3]

Using their N-methylated peptides, Pratim Bose et al. found that the increasing extent of methylation increased the efficiency of the peptides against Aβ-mediated toxicity in the MTT assay in nondifferentiated PC-12 cells.[1] In work using PC-12 cells and other neuronal cell lines, it is important to note whether the cells are differentiated into a neuronal phenotype because not all laboratories take care to do that. In nondifferentiated cells, measurements of toxicity and its inhibition are still valid, but they are not relevant to neurons. If the goal is to test inhibition of neurotoxicity, as opposed to general cytotoxicity, the cells should be differentiated into a neuronal phenotype.

The Aβ(32−37) analogues were not toxic themselves and the trimethylated and pentamethylated peptides were the most efficient inhibitors of Aβ42-induced toxicity in the study by Pratim Bose et al.[1] Treatment with the pentamethylated peptide 4 at 5-fold excess to Aβ42 did not differ from the untreated condition. The pentamethylated peptide also was found to increase longevity and improve locomotion in a *Drosophila melanogaster* model expressing Aβ42 in the central nervous system. This effect likely was mediated by the action of the peptide on Aβ42 because no effect on lifespan was observed in wild-type flies treated with this peptide.[1] As mentioned above, all of the 41 Aβ(32−37) analogues tested by Bansal et al. in the MTT assay in nondifferentiated PC-12 cells were weaker inhibitors of Aβ40-induced toxicity than the parent peptide,[35] suggesting that sequence alterations reduce the ability of the fragment to bind Aβ42, as opposed to the N-methylation used by Pratim Bose et al.

Pr-IIGL$_a$ and RIIGL$_a$ were evaluated using the MTT assay in differentiated SH-SY5Y human neuroblastoma cells. RIIGL$_a$ inhibited the cytotoxic effect of Aβ42 significantly. In contrast, Pr-IIGL$_a$ was found to be toxic and consequently did not exert a protective effect.[36] An Aβ(38−42) analogue tested by the same group, RVVIA-NH$_2$, tended toward protecting against toxicity, but the effect was mild and not statistically significant.[38]

In the initial screen by our group, four peptides showed the highest inhibitory potential: Aβ(30−42), Aβ(31−42), Aβ(39−42), and Aβ(30−40).[3,30] Because Aβ(30−42) and Aβ(31−42) are highly similar, we decided to characterize further only the stronger inhibitor of the two, Aβ(31−42). Thus, we focused on Aβ(31−42), Aβ(39−42), and Aβ(30−40). Aβ(31−42) was found to be the strongest inhibitor of Aβ42-induced neurotoxicity in differentiated PC-12 cells with IC$_{50}$ values of 14 ± 2 and 20 ± 4 μM in MTT reduction and lactate dehydrogenase (LDH) release assays, respectively.[30] In the same assays, the IC$_{50}$ values for Aβ(39−42) were 16 ± 5 and 47 ± 14 μM,[30] and for Aβ(30−40) 34 ± 12 μM and 29 ± 4 μM, respectively.[4]

Because AD is thought to initiate as a disease of synapses before overt neuron loss occurs,[48] we assessed further the effect of these CTFs on Aβ42-induced synaptic toxicity. A decrease in the frequency of spontaneous miniature excitatory postsynaptic currents (mEPSC) reflects a decline in the number of functional excitatory synapses or a reduction in presynaptic release probability. We used Aβ-induced attenuation of mEPSC frequency in primary mouse hippocampal neurons to determine whether Aβ(31−42), Aβ(39−42), and Aβ(30−40) rescued Aβ42-mediated synaptotoxicity. Significant inhibition of Aβ42-induced toxicity was observed already at a 1:1 Aβ42/Aβ(31−42) concentration ratio, and at 10-fold excess, Aβ(31−42) rescued mEPSC deficits back to baseline,[30] demonstrating that this CTF not only protected neurons against Aβ42-induced cytotoxicity but also protected synaptic function from toxic insults by Aβ42. Aβ(30−40) showed a similar effect,[4] whereas the protective activity of Aβ(39−42) was lower yet still statistically significant ($P < 0.05$) at 10-fold excess relative to Aβ42.[30]

Electrophysiological experiments, using coronal slices of rat primary motor cortex, demonstrated that RIIGL$_a$ prevented the attenuation of the field excitatory postsynaptic potential by Aβ42. In contrast, RVVIA-NH$_2$ did not affect Aβ42-induced synaptotoxicity. In *in vivo* experiments using extracellular single-unit recordings combined with iontophoresis in wild-type male Wistar rats, RIIGL$_a$ protected neurons from the NMDA's response-enhancing effect of Aβ42 in the hippocampal CA1 region, whereas RVVIA-NH$_2$ was ineffective.[38] This latter result contrasted with data from our groups showing a protective effect for VVIA-NH$_2$ (see below), suggesting that the addition of arginine at position 35 abolished the protective effect of this peptide.

Investigation of the specificity of Aβ(39−42) and the mechanism(s) by which it exerts its protective activity suggested that the effect of this tetrapeptide was specific for Aβ because Aβ(39−42) did not inhibit the toxicity induced by other toxins, such as staurosporine, a nonselective protein-kinase inhibitor that induces apoptosis in multiple cell types, alamethicin, a fungal peptide antibiotic that potentially induces voltage-dependent ion-channel formation in phospholipid membranes, or α-synuclein, an amyloidogenic protein associated with Parkinson's disease and other synucleinopathies.[27] However, the effect of Aβ(39−42) was not specific to Aβ42 because the tetrapeptide also inhibited Aβ40-induced toxicity with similar efficacy.[49] These data suggested that although Aβ(39−42) inhibits Aβ toxicity via directly and specifically interacting with the full-length peptide, the interaction likely is not with the C-terminus, which differs between Aβ40 and Aβ42.

DOI: 10.1021/acschemneuro.6b00154
ACS Chem. Neurosci. XXXX, XXX, XXX−XXX

We examined potential correlations among the different data sets, including inhibition of hexamer formation, abundance of Aβ42 P_2 particles, toxicity inhibition, solubility, β-sheet formation, and CTF particle growth. The analysis showed that inhibition of Aβ42 hexamer formation correlated relatively highly with CTF solubility, β-sheet formation, and particle size increase, but not with inhibition of Aβ42-induced toxicity. Inhibition of Aβ42-induced toxicity also did not correlate with CTF biophysical properties but correlated with decreased abundance of P_2 particles after the first day of measurement, suggesting that P_2 oligomers are the main form of Aβ42 causing neurotoxicity.

To gain a deeper insight into the way the CTFs interact with Aβ42, Aβ42 oligomer formation was modeled in the absence or presence of Aβ(31−42), Aβ(39−42), or Aβ(30−40) using discrete molecular dynamics (DMD), and interactions that correlated with inhibition of Aβ42 toxicity were delineated.[50] CTFs coassembled with Aβ42 into large hetero-oligomers containing multiple Aβ42 and CTF molecules. All three CTFs decreased Aβ42's β-strand-formation propensity concentration-dependently, suggesting that a lower β-sheet content correlated with decreased toxicity. CTFs had a high binding propensity to the hydrophobic regions of Aβ42. Interestingly, only CTFs, but not Aβ(21−30), which was used as a control, were found to bind the Aβ42 region Aβ(2−4). Consequently, only CTFs reduced the solvent accessibility of Aβ42 in the region Aβ(1−5). Because the control fragment did not inhibit Aβ42 toxicity, these findings suggested that the region Aβ(1−5), which also was more solvent exposed in Aβ42 than in Aβ40 oligomers, is involved in mediating Aβ42-induced neurotoxicity.[50]

Subsequent experiments examining potential binding of Aβ(39−42) to different regions in Aβ42 used tyrosine-substituted Aβ42 at different single sites and measured the intrinsic fluorescence variation surrounding the tyrosine residue upon addition of Aβ(39−42). These experiments showed that the inhibitor favored interaction at Aβ42 N-terminus,[27] consistent with the DMD simulation data.[50]

Ion mobility−mass spectrometry (IM−MS) experiments showed that Aβ(39−42) prevented the formation of Aβ42 decamers and dodecamers and removed these structures from solution.[49] Interestingly, in contrast, Aβ(39−42) did not change the oligomer size distribution of Aβ40,[49] suggesting some specificity for Aβ42. Surprisingly, though Aβ(39−42) shifted the oligomer size distribution of Aβ42, it did not interrupt fibril formation by Aβ40 or Aβ42, as evidenced by ThT fluorescence measurements and morphological examination by EM.[49] These results suggest that decamers and dodecamers of Aβ42 correlate most closely with toxicity, whereas smaller oligomers and fibrils presumably are weakly toxic or nontoxic. The decamers and dodecamers observed in the IM−MS are substantially smaller[51] than the P_2 particles observed by DLS.[4] Thus, although direct comparison between these two types of oligomers is difficult due to the very different experimental conditions, the observation that both types of oligomers correlated with toxicity suggests that the decamers and dodecamers may be precursors of the 20−60 nm P_2 particles.

Most lines of evidence suggest that CTFs do not prevent Aβ42 monomers from binding to each other but rather coassemble with Aβ42 into nontoxic hetero-oligomers. Inhibition of Aβ42 toxicity by CTFs correlates with accumulation of P_1 hetero-oligomers, suggesting attenuation of P_1-to-P_2 conversion. This putative mechanism is shown in Figure 8.[4] In the absence of CTFs (Figure 8, top path), Aβ monomers rapidly self-assemble into small oligomers (P_1 particles). Association of these oligomers into larger assemblies (P_2 particles) is relatively slow, whereas the conversion of P_2 assemblies into fibrils or their disassembly back into P_1 oligomers is fast. As a result, little accumulation of P_2 particles is observed. In the presence of CTFs (Figure 8, bottom path), Aβ42 and the CTFs coassemble into hetero-oligomers, the size of which cannot be distinguished from that of the oligomers formed in the absence of CTFs by low-resolution methods, such as DLS or EM. The CTFs stabilize both P_1 and P_2 oligomers and delay the conversion of P_2 assemblies into fibrils. However, CTFs vary in their effects on the conversion of the small P_1 oligomers into the larger P_2 oligomers. Effective inhibitors slow this process and give rise predominantly to P_1 oligomers, whereas less effective inhibitors may allow for a relatively fast P_1-to-P_2 conversion. Thus, the reverse correlation between P_2 abundance and toxicity inhibition suggests that a predominant mechanism by which CTFs inhibit Aβ42 toxicity is stabilization of P_1 hetero-oligomers. Other distinctions between effective and ineffective inhibitors are in the fine details of the hetero-oligomers themselves as exemplified by the Aβ(39−42) variants discussed below.

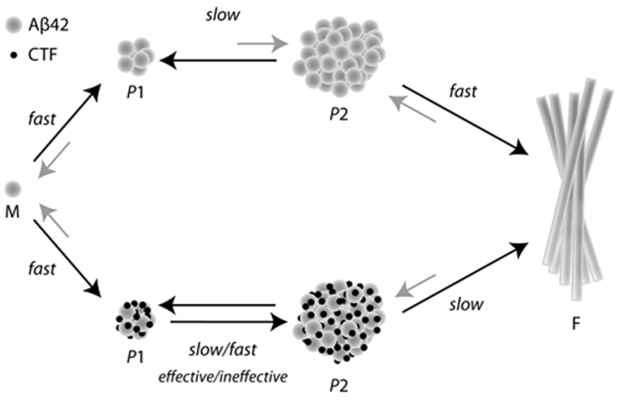

Figure 8. Schematic representation of a putative mechanism by which CTFs affect Aβ42 assembly. Monomer (M) assembly into P_1 particles is a faster process in the absence (top path) than in the presence (bottom path) of CTFs. CTFs may accelerate the conversion of P_1 into P_2 oligomers, but effective inhibitors of Aβ42-induced toxicity induce smaller acceleration than ineffective ones, shifting the population toward P_1. All CTFs slow the maturation of P_2 assemblies into fibrils (F). Reproduced from ref 4. Copyright 2010 American Chemical Society.

STRUCTURE−ACTIVITY RELATIONSHIP STUDIES OF C-TERMINAL FRAGMENT DERIVATIVES

Peptides possess several favorable properties as drug candidates, such as higher potency, higher selectivity, and better safety than nonpeptidic small-molecule drugs, but their short half-lives and low bioavailability challenge their transformation into drugs.[52] During the past decade, attention has been focused increasingly on the potential therapeutic use of peptides, and more peptide-based drugs were approved relative to previous decades.[52] To be used as a drug, most peptides need to be structurally modified, for example, by N-methylation, as was done by the Arvidsson group,[1,34] to improve their efficacy, stability, and bioavailability. As initial steps toward improving "druggability", our group used different strategies to modify Aβ(31−42) and

DOI: 10.1021/acschemneuro.6b00154
ACS Chem. Neurosci. XXXX, XXX, XXX−XXX

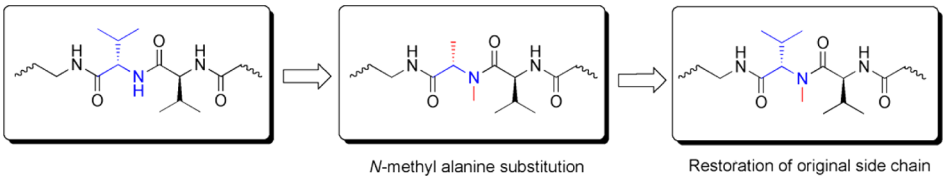

Figure 9. Schematic diagram of our group's two-step N-methylation strategy for Aβ(31−42) SAR studies. Reproduced from ref 2. Copyright 2012 Wiley-VCH Verlag GmbH & Co. KGaA.

Table 2. Aβ(31−42) Derivatives and Their Inhibitory Activity against Aβ42-Induced Toxicity

code	sequence	solubility (μM)	IC_{50}(MTT) (μM)	IC_{50}(LDH) (μM)
Aβ(31−42)	IIGLMVGGVVIA	25 ± 4	18 ± 1	43 ± 2
[*N*-Me-A1]Aβ(31−42)	**(*N*-Me)A**-IGLMVGGVVIA	8 ± 1		
[*N*-Me-A2]Aβ(31−42)	I-**(*N*-Me)A**-GLMVGGVVIA	101 ± 18		
[*N*-Me-A3]Aβ(31−42)	II-**(*N*-Me)A**-LMVGGVVIA	102 ± 16	18 ± 1	34 ± 3
[*N*-Me-A4]Aβ(31−42)	IIG-**(*N*-Me)A**-MVGGVVIA	127 ± 37		
[*N*-Me-A5]Aβ(31−42)	IIGL-**(*N*-Me)A**-VGGVVIA	105 ± 20		
[*N*-Me-A6]Aβ(31−42)	IIGLM-**(*N*-Me)A**-GGVVIA	87 ± 18		
[*N*-Me-A7]Aβ(31−42)	IIGLMV-**(*N*-Me)A**-GVVIA	88 ± 14		
[*N*-Me-A8]Aβ(31−42)	IIGLMVG-**(*N*-Me)A**-VVIA	41 ± 12	12 ± 1	14 ± 1
[*N*-Me-A9]Aβ(31−42)	IIGLMVGG-**(*N*-Me)A**-VIA	115 ± 21	6 ± 1	7 ± 1
[*N*-Me-A10]Aβ(31−42)	IIGLMVGGV-**(*N*-Me)A**-IA	121 ± 28		
[*N*-Me-A11]Aβ(31−42)	IIGLMVGGVV-**(*N*-Me)A**-A	86 ± 22	10 ± 1	37 ± 3
[*N*-Me-A12]Aβ(31−42)	IIGLMVGGVVI-**(*N*-Me)A**	28 ± 13		
[*N*-Me-I1]Aβ(31−42)	**(*N*-Me)I**-IGLMVGGVVIA	7 ± 1		
[*N*-Me-G3]Aβ(31−42)	II-**(*N*-Me)G**-LMVGGVVIA	118 ± 11	26 ± 1	*a*
[*N*-Me-G8]Aβ(31−42)	IIGLMVG-**(*N*-Me)G**-VVIA	18 ± 2	28 ± 1	71 ± 20
[*N*-Me-V9]Aβ(31−42)	IIGLMVGG-**(*N*-Me)V**-VIA	136 ± 18	6 ± 1	67 ± 8
[*N*-Me-I11]Aβ(31−42)	IIGLMVGGVV-**(*N*-Me)I**-A	132 ± 34	13 ± 1	49 ± 3

[a]No inhibition.

Aβ(39−42) systematically, to determine key structural characteristics important for their inhibitory activity. In both cases, we found that the inhibitory activities of these peptides were controlled by specific structural characteristics and could be improved.

Aβ(31−42) is a hydrophobic peptide with relatively low aqueous solubility, which makes assessing its inhibitory and assembly characteristics difficult. To tackle these challenges in a systematic way, we used a two-step N-methylation strategy.[2] First, each residue was substituted by *N*-Me-alanine (*N*-Me-A) and the inhibitory activity of each derivative was tested. In the next step, in positions where substitution produced a significant effect on the inhibitory activity, we restored the original side chain (Figure 9). This strategy allowed exploration of the roles of both *N*-Me substitution and side-chain structure in mediating inhibitory activity. We found that introducing an *N*-Me amino acid effectively increased the aqueous solubility and the inhibitory activity of Aβ(31−42) (Table 2). In particular, N-methylation at position 9 or 11 increased the inhibitory activity in the MTT assay by 3-fold or 2-fold, respectively, relative to the parent peptide. Comparing our singly N-methylated Aβ(31−42) derivatives to the multiply N-methylated Aβ(32−37) peptides,[1,34] our systematic strategy allowed determination of the key positions and structures controlling the inhibitory activity of Aβ(31−42). Due to different conditions in toxicity inhibition experiments, that is, the use of nondifferentiated PC-12 versus differentiated PC-12 cells and 1:5 versus 1:10 Aβ42/CTF concentration ratios, used in experiments by Pratim Bose et al. versus our experiments, respectively, direct comparison of the two studies is difficult.

The N-methylated peptides of Pratim Bose et al. showed improved bioavailability relative to the nonmethylated parent peptide.[34] The authors tested solubility, lipophilicity, stability to enzymatic degradation, and permeability to assess the potential of the N-methylated peptides as drug candidates. By ultra-performance liquid chromatography with both UV and MS detection, estimated log *D* was calculated, and the lipophilicity of peptides 1−4 was found to increase, expectedly, with increasing extent of methylation.[34] Peptides with N-methylation at least at every other peptide bond were resistant to degradation by Pronase for up to 24 h of testing.[34] In contrast, permeability of peptides across an epithelial cell monolayer decreased with increasing extent of N-methylation.[34] Peptide 4, for example, had the lowest permeability in the series. Nonetheless, apparently, the permeability of this peptide was sufficient for a protective effect in a *Drosophila* model.[1] The success of N-methylated peptides in increasing bioavailability and inhibitory activity against Aβ42-induced toxicity highlights their potential as drug leads for AD.

Because Aβ(39−42) had substantially higher aqueous solubility than Aβ(31−42), improvement of solubility was not a high priority and a different strategy was used for SAR studies. A series of Aβ(39−42) derivatives, including alanine substitution of the first three residues (**AVIA**, V**A**IA, VV**AA**), an inverso-peptide (vvia, lower-case letters represent D-configuration), N-terminally and C-terminally protected analogues (Ac-VVIA, VVIA-NH_2), a retropeptide (AIVV), and N-terminally and C-terminally protected versions of the retropeptide (Ac-AIVV, AIVV-NH_2)[27] (Table 3) were synthesized. Screening the inhibitory activity showed that the side chains of

DOI: 10.1021/acschemneuro.6b00154
ACS Chem. Neurosci. XXXX, XXX, XXX−XXX

Table 3. Aβ(39−42) Derivatives and Their Inhibitory Activity against Aβ42-Induced Toxicity

sequence	IC_{50}(MTT) (μM)	IC_{50}(LDH) (μM)
VVIA	21 ± 6	16 ± 3
AVIA	53 ± 10	22 ± 5
V**A**IA	15 ± 3	14 ± 2
VV**A**A	*b*	*b*
vvia[a]	*b*	*b*
Ac-VVIA	*b*	*b*
VVIA-$\mathbf{NH_2}$	28 ± 7	30 ± 5
AIVV	14 ± 1	22 ± 3
Ac-AIVV	*b*	*b*
AIVV-$\mathbf{NH_2}$	20 ± 4	16 ± 3

[a]Lower-case letters represent D-configuration. [b]Inactive.

Val39 and Val40 were relatively insensitive to structural changes, whereas the Ile41 side chain was important for inhibiting toxicity. However, the observation that inhibitory activity was maintained in the retro-sequence, AIVV, suggested that the bulky hydrophobic side chain in position 41, such as Ile or Val, might be sufficient for the inhibitory activity. Loss of activity in the inverso-peptide (vvia) indicated that the chirality of Aβ(39−42) was required for inhibitory activity. The N-terminally acetylated analogues, Ac-VVIA and Ac-AIVV, showed no inhibitory activity, whereas the C-terminally amidated analogues, VVIA-NH_2 and AIVV-NH_2, were as active as Aβ(39−42), suggesting that electrostatic interactions between the positively charged N-terminus of the CTF and the negatively charged full-length peptide (total charge = −3) contributed substantially to the binding of Aβ(39−42) and its derivatives to Aβ42 and to the inhibitory activity of CTFs. The fact that the C-terminus could be amidated suggested that this could be a viable strategy for protecting Aβ(39−42) from carboxypeptidases.

Interactions of the N- and C-terminally modified forms of Aβ(39−42) with Aβ42 recently were investigated using IM−MS.[53] The active inhibitor, VVIA-NH_2, bound directly to Aβ42 monomer and small oligomers, whereas the inactive derivative, Ac-VVIA, bound only to Aβ42 monomers. VVIA-NH_2 inhibited Aβ dodecamer formation and disaggregated preformed Aβ42 dodecamers, as was observed previously for Aβ(39−42).[49] In contrast, Ac-VVIA appeared to induce transformation of Aβ42 dodecamers into larger aggregates.[53] Molecular dynamics simulations suggested that the binding of Ac-VVIA to the Aβ42 C-terminus was slightly reduced compared with Aβ(39−42), whereas the binding of VVIA-NH_2 to the Aβ42 C-terminus was increased substantially relative to Aβ(39−42), suggesting that binding to the C-terminus is important for inhibition of Aβ42-induced toxicity by these CTFs. Neither Aβ(39−42),[49] Ac-VVIA nor VVIA-NH_2[53] inhibited Aβ42 fibril formation, strongly supporting the hypothesis that oligomers rather than fibrils are responsible for Aβ toxicity.

CONCLUSIONS

As evidence emerged ascribing pathogenic primacy to Aβ oligomers rather than fibrils, inhibitor design efforts shifted toward inhibition of Aβ oligomerization. Aβ42 oligomers are a particularly attractive target because Aβ42 is more toxic than Aβ40, even though the shorter form is ∼10-times more abundant in the brain. Guided by the principle of self-recognition and considering the critical role of the Aβ42 C-terminus in self-assembly, several groups including our own, have explored C-terminal Aβ fragments as inhibitors of Aβ oligomerization and neurotoxicity. Many of the CTFs showed potent activity. However, the relationship between inhibition of oligomerization and inhibition of neurotoxicity is complex, and a good oligomerization inhibitor is not necessarily a good toxicity inhibitor. As discussed earlier, CTFs likely coassemble with Aβ42 and form hetero-oligomers that are not toxic. Other inhibitors, including various peptides and small molecules, have been reported to use similar mechanisms for inhibition of Aβ toxicity, that is, binding to and co-oligomerizing with Aβ42 to form nontoxic structures.[12,54−56] Due to the complexity of the relationship between assembly and toxicity inhibition, using assembly inhibition as a strategy for drug design should be considered with caution. Though peptide-based Aβ aggregation inhibitors have been studied for about 20 years now, several key unsolved questions can hinder the drug discovery processes: (1) Why are Aβ oligomers toxic? (2) How could the oligomers' toxicity be blocked? (3) What are the best procedures to test inhibitors of Aβ oligomer toxicity that can be translated from the test tube to the patients? (4) If a peptide inhibitor can self-aggregate, which form(s) of it is active and how can inhibitor homogeneity be controlled? (5) Would a strategy based on hetero-oligomerization of CTFs with Aβ42 potentially work *in vivo* if it does not prevent fibril formation, and will the formation of nontoxic hetero-oligomers allow for clearance of Aβ before it forms fibrils? Most of these questions are relevant to both peptide drugs and small-molecule drugs using similar inhibitory mechanisms. Understanding the fundamental questions and building appropriate evaluation systems is necessary for efficient discovery of active compounds. Potent and weak inhibitors can serve as tools for understanding such fundamental questions. With the advantage of many potent compounds and structural varieties thereof, finding peptide-based drugs as Aβ assembly and toxicity inhibitors holds promise for therapy development and enhanced mechanistic understanding of the underlying pathology of AD.

AUTHOR INFORMATION

Corresponding Author

*G.B. Phone: 310-206 2082. Fax: 310-206 1700. E-mail: gbitan@mednet.ucla.edu.

Funding

The work was supported by NIH/NIA Grant R01AG050721, RGK Foundation Grant 20143057, Michael J. Fox Foundation Grant 10220, Cure Alzheimer's Fund Grant 20152631, The UCLA Mary S. Easton Endowment, and a Grant from Team Parkinson/Parkinson Alliance.

Notes

The authors declare no competing financial interest.

REFERENCES

(1) Pratim Bose, P., Chatterjee, U., Nerelius, C., Govender, T., Norstrom, T., Gogoll, A., Sandegren, A., Gothelid, E., Johansson, J., and Arvidsson, P. I. (2009) Poly-N-methylated amyloid β-peptide (Aβ) C-terminal fragments reduce Aβ toxicity in vitro and in *Drosophila melanogaster*. *J. Med. Chem. 52*, 8002−8009.

(2) Li, H., Zemel, R., Lopes, D. H., Monien, B. H., and Bitan, G. (2012) A two-step strategy for structure-activity relationship studies of N-methylated Aβ42 C-terminal fragments as Aβ42 toxicity inhibitors. *ChemMedChem 7*, 515−522.

(3) Li, H., Monien, B. H., Fradinger, E. A., Urbanc, B., and Bitan, G. (2010) Biophysical characterization of Aβ42 C-terminal fragments: inhibitors of Aβ42 neurotoxicity. *Biochemistry 49*, 1259−1267.

DOI: 10.1021/acschemneuro.6b00154
ACS Chem. Neurosci. XXXX, XXX, XXX−XXX

(4) Li, H., Monien, B. H., Lomakin, A., Zemel, R., Fradinger, E. A., Tan, M., Spring, S. M., Urbanc, B., Xie, C. W., Benedek, G. B., and Bitan, G. (2010) Mechanistic investigation of the inhibition of Aβ42 assembly and neurotoxicity by Aβ42 C-terminal fragments. *Biochemistry 49*, 6358−6364.
(5) Glenner, G. G. (1989) Amyloid β protein and the basis for Alzheimer's disease. *Prog. Clin Biol. Res. 317*, 857−868.
(6) Nussbaum, R. L., and Polymeropoulos, M. H. (1997) Genetics of Parkinson's disease. *Hum. Mol. Genet. 6*, 1687−1691.
(7) Walling, H. W., Baldassare, J. J., and Westfall, T. C. (1998) Molecular aspects of Huntington's disease. *J. Neurosci. Res. 54*, 301−308.
(8) Riedl, L., Mackenzie, I. R., Forstl, H., Kurz, A., and Diehl-Schmid, J. (2014) Frontotemporal lobar degeneration: current perspectives. *Neuropsychiatr. Dis. Treat. 10*, 297−310.
(9) Hikida, T., Gamo, N. J., and Sawa, A. (2012) DISC1 as a therapeutic target for mental illnesses. *Expert Opin. Ther. Targets 16*, 1151−1160.
(10) Buhimschi, I. A., Nayeri, U. A., Zhao, G., Shook, L. L., Pensalfini, A., Funai, E. F., Bernstein, I. M., Glabe, C. G., and Buhimschi, C. S. (2014) Protein misfolding, congophilia, oligomerization, and defective amyloid processing in preeclampsia. *Sci. Transl. Med. 6*, 245ra292.
(11) Wood, S. J., Wetzel, R., Martin, J. D., and Hurle, M. R. (1995) Prolines and amyloidogenicity in fragments of the Alzheimer's peptide β/A4. *Biochemistry 34*, 724−730.
(12) Rahimi, F., Li, H., Sinha, S., and Bitan, G. (2016) Modulators of amyloid β-protein (Aβ) self-assembly, in *Developing Therapeutics for Alzheimer's Disease* (Wolfe, M. S., Ed.), pp 97−191, Elsevier, Amsterdam.
(13) Hardy, J. A., and Higgins, G. A. (1992) Alzheimer's disease: the amyloid cascade hypothesis. *Science 256*, 184−185.
(14) Kirkitadze, M. D., Bitan, G., and Teplow, D. B. (2002) Paradigm shifts in Alzheimer's disease and other neurodegenerative disorders: The emerging role of oligomeric assemblies. *J. Neurosci. Res. 69*, 567−577.
(15) Haass, C., and Selkoe, D. J. (2007) Soluble protein oligomers in neurodegeneration: lessons from the Alzheimer's amyloid β-peptide. *Nat. Rev. Mol. Cell Biol. 8*, 101−112.
(16) Rahimi, F., and Bitan, G. (2012) The structure and function of fibrillar and oligomeric assemblies of amyloidogenic proteins, in *Non-fibrillar amyloidogenic protein assemblies—common cytotoxins underlying degenerative diseases* (Rahimi, F., and Bitan, G., Eds.), pp 1−36, Springer Science+Media B.V., Dordrecht.
(17) Bitan, G., Kirkitadze, M. D., Lomakin, A., Vollers, S. S., Benedek, G. B., and Teplow, D. B. (2003) Amyloid β-protein (Aβ) assembly: Aβ40 and Aβ42 oligomerize through distinct pathways. *Proc. Natl. Acad. Sci. U. S. A. 100*, 330−335.
(18) Bitan, G., Tarus, B., Vollers, S. S., Lashuel, H. A., Condron, M. M., Straub, J. E., and Teplow, D. B. (2003) A molecular switch in amyloid assembly: Met^{35} and amyloid β-protein oligomerization. *J. Am. Chem. Soc. 125*, 15359−15365.
(19) Sgourakis, N. G., Yan, Y., McCallum, S. A., Wang, C., and Garcia, A. E. (2007) The Alzheimer's peptides Aβ40 and 42 adopt distinct conformations in water: a combined MD/NMR study. *J. Mol. Biol. 368*, 1448−1457.
(20) Urbanc, B., Cruz, L., Yun, S., Buldyrev, S. V., Bitan, G., Teplow, D. B., and Stanley, H. E. (2004) *In silico* study of amyloid β-protein folding and oligomerization. *Proc. Natl. Acad. Sci. U. S. A. 101*, 17345−17350.
(21) Murakami, K. (2014) Conformation-specific antibodies to target amyloid β oligomers and their application to immunotherapy for Alzheimer's disease. *Biosci., Biotechnol., Biochem. 78*, 1293−1305.
(22) Sampson, W. R., Patsiouras, H., and Ede, N. J. (1999) The synthesis of 'difficult' peptides using 2-hydroxy-4-methoxybenzyl or pseudoproline amino acid building blocks: a comparative study. *J. Pept. Sci. 5*, 403−409.
(23) Ajikumar, P. K., and Devaky, K. S. (2001) Solid phase synthesis of hydrophobic difficult sequence peptides on BDDMA-PS support. *J. Pept. Sci. 7*, 641−649.
(24) Nilsson, M. R., Nguyen, L. L., and Raleigh, D. P. (2001) Synthesis and purification of amyloidogenic peptides. *Anal. Biochem. 288*, 76−82.
(25) Tickler, A. K., Clippingdale, A. B., and Wade, J. D. (2004) Amyloid-β as a "difficult sequence" in solid phase peptide synthesis. *Protein Pept. Lett. 11*, 377−384.
(26) Condron, M. M., Monien, B. H., and Bitan, G. (2008) Synthesis and purification of highly hydrophobic peptides derived from the C-terminus of amyloid β-protein. *Open Biotechnol. J. 2*, 87−93.
(27) Li, H., Du, Z., Lopes, D. H., Fradinger, E. A., Wang, C., and Bitan, G. (2011) C-Terminal tetrapeptides inhibit Aβ42-induced neurotoxicity primarily through specific interaction at the N-Terminus of Aβ42. *J. Med. Chem. 54*, 8451−8460.
(28) Palasek, S. A., Cox, Z. J., and Collins, J. M. (2007) Limiting racemization and aspartimide formation in microwave-enhanced Fmoc solid phase peptide synthesis. *J. Pept. Sci. 13*, 143−148.
(29) Chan, W. C., and White, P. D. (2000) *Fmoc solid phase peptide synthesis: A practical approach*, Oxford University Press, New York.
(30) Fradinger, E. A., Monien, B. H., Urbanc, B., Lomakin, A., Tan, M., Li, H., Spring, S. M., Condron, M. M., Cruz, L., Xie, C. W., Benedek, G. B., and Bitan, G. (2008) C-terminal peptides coassemble into Aβ42 oligomers and protect neurons against Aβ42-induced neurotoxicity. *Proc. Natl. Acad. Sci. U. S. A. 105*, 14175−14180.
(31) Takano, K., Endo, S., Mukaiyama, A., Chon, H., Matsumura, H., Koga, Y., and Kanaya, S. (2006) Structure of amyloid β fragments in aqueous environments. *FEBS J. 273*, 150−158.
(32) Lansbury, P. T., Jr., Costa, P. R., Griffiths, J. M., Simon, E. J., Auger, M., Halverson, K. J., Kocisko, D. A., Hendsch, Z. S., Ashburn, T. T., Spencer, R. G., et al. (1995) Structural model for the β-amyloid fibril based on interstrand alignment of an antiparallel-sheet comprising a C-terminal peptide. *Nat. Struct. Biol. 2*, 990−998.
(33) Petkova, A. T., Ishii, Y., Balbach, J. J., Antzutkin, O. N., Leapman, R. D., Delaglio, F., and Tycko, R. (2002) A structural model for Alzheimer's β-amyloid fibrils based on experimental constraints from solid state NMR. *Proc. Natl. Acad. Sci. U. S. A. 99*, 16742−16747.
(34) Bose, P. P., Chatterjee, U., Hubatsch, I., Artursson, P., Govender, T., Kruger, H. G., Bergh, M., Johansson, J., and Arvidsson, P. I. (2010) In vitro ADMET and physicochemical investigations of poly-N-methylated peptides designed to inhibit Aβ aggregation. *Bioorg. Med. Chem. 18*, 5896−5902.
(35) Bansal, S., Maurya, I. K., Yadav, N., Thota, C. K., Kumar, V., Tikoo, K., Chauhan, V. S., and Jain, R. (2016) C-Terminal fragment, $Aβ_{32-37}$, analogues protect against Aβ aggregation-induced toxicity. *ACS Chem. Neurosci. 7*, 615−623.
(36) Fülöp, L., Zarandi, M., Datki, Z., Soos, K., and Penke, B. (2004) β-amyloid-derived pentapeptide RIIGLa inhibits Aβ(1−42) aggregation and toxicity. *Biochem. Biophys. Res. Commun. 324*, 64−69.
(37) Laskay, G., Zarandi, M., Varga, J., Jost, K., Fonagy, A., Torday, C., Latzkovits, L., and Penke, B. (1997) A putative tetrapeptide antagonist prevents β-amyloid-induced long-term elevation of $[Ca^{2+}]_i$ in rat astrocytes. *Biochem. Biophys. Res. Commun. 235*, 479−481.
(38) Szegedi, V., Fülöp, L., Farkas, T., Rozsa, E., Robotka, H., Kis, Z., Penke, Z., Horvath, S., Molnar, Z., Datki, Z., Soos, K., Toldi, J., Budai, D., Zarandi, M., and Penke, B. (2005) Pentapeptides derived from Aβ1−42 protect neurons from the modulatory effect of Aβ fibrils—an in vitro and in vivo electrophysiological study. *Neurobiol. Dis. 18*, 499−508.
(39) Harkany, T., Abraham, I., Laskay, G., Timmerman, W., Jost, K., Zarandi, M., Penke, B., Nyakas, C., and Luiten, P. G. (1999) Propionyl-IIGL tetrapeptide antagonizes β-amyloid excitotoxicity in rat nucleus basalis. *NeuroReport 10*, 1693−1698.
(40) Bitan, G., Lomakin, A., and Teplow, D. B. (2001) Amyloid β-protein oligomerization: prenucleation interactions revealed by photo-induced cross-linking of unmodified proteins. *J. Biol. Chem. 276*, 35176−35184.
(41) Bitan, G. (2006) Structural study of metastable amyloidogenic protein oligomers by photo-induced cross-linking of unmodified proteins. *Methods Enzymol. 413*, 217−236.

DOI: 10.1021/acschemneuro.6b00154
ACS Chem. Neurosci. XXXX, XXX, XXX−XXX

(42) Fancy, D. A., and Kodadek, T. (1999) Chemistry for the analysis of protein-protein interactions: Rapid and efficient cross-linking triggered by long wavelength light. *Proc. Natl. Acad. Sci. U. S. A. 96*, 6020−6024.
(43) Bitan, G., and Teplow, D. B. (2005) Preparation of aggregate-free, low molecular weight amyloid-β for assembly and toxicity assays. *Methods Mol. Biol. 299*, 3−9.
(44) Abe, K., and Saito, H. (1998) Amyloid β protein inhibits cellular MTT reduction not by suppression of mitochondrial succinate dehydrogenase but by acceleration of MTT formazan exocytosis in cultured rat cortical astrocytes. *Neurosci. Res. 31*, 295−305.
(45) Datki, Z., Juhasz, A., Galfi, M., Soos, K., Papp, R., Zadori, D., and Penke, B. (2003) Method for measuring neurotoxicity of aggregating polypeptides with the MTT assay on differentiated neuroblastoma cells. *Brain Res. Bull. 62*, 223−229.
(46) Shearman, M. S., Ragan, C. I., and Iversen, L. L. (1994) Inhibition of PC12 cell redox activity is a specific, early indicator of the mechanism of β-amyloid-mediated cell death. *Proc. Natl. Acad. Sci. U. S. A. 91*, 1470−1474.
(47) Pereira, C., Santos, M. S., and Oliveira, C. (1998) Mitochondrial function impairment induced by amyloid β-peptide on PC12 cells. *NeuroReport 9*, 1749−1755.
(48) Walsh, D. M., and Selkoe, D. J. (2004) Oligomers on the brain: the emerging role of soluble protein aggregates in neurodegeneration. *Protein Pept. Lett. 11*, 213−228.
(49) Gessel, M. M., Wu, C., Li, H., Bitan, G., Shea, J. E., and Bowers, M. T. (2012) Aβ(39−42) modulates Aβ oligomerization but not fibril formation. *Biochemistry 51*, 108−117.
(50) Urbanc, B., Betnel, M., Cruz, L., Li, H., Fradinger, E. A., Monien, B. H., and Bitan, G. (2011) Structural basis for Aβ(1−42) toxicity inhibition by Aβ C-terminal fragments: discrete molecular dynamics study. *J. Mol. Biol. 410*, 316−328.
(51) Bernstein, S. L., Dupuis, N. F., Lazo, N. D., Wyttenbach, T., Condron, M. M., Bitan, G., Teplow, D. B., Shea, J. E., Ruotolo, B. T., Robinson, C. V., and Bowers, M. T. (2009) Amyloid-β protein oligomerization and the importance of tetramers and dodecamers in the aetiology of Alzheimer's disease. *Nat. Chem. 1*, 326−331.
(52) Craik, D. J., Fairlie, D. P., Liras, S., and Price, D. (2013) The future of peptide-based drugs. *Chem. Biol. Drug Des. 81*, 136−147.
(53) Zheng, X., Wu, C., Liu, D., Li, H., Bitan, G., Shea, J. E., and Bowers, M. T. (2016) Mechanism of C-terminal fragments of amyloid β-protein as Aβ inhibitors: Do C-terminal interactions play a key role in their inhibitory activity? *J. Phys. Chem. B 120*, 1615−1623.
(54) McLaurin, J., Golomb, R., Jurewicz, A., Antel, J. P., and Fraser, P. E. (2000) Inositol stereoisomers stabilize an oligomeric aggregate of Alzheimer amyloid β peptide and inhibit Aβ-induced toxicity. *J. Biol. Chem. 275*, 18495−18502.
(55) Kai, T., Zhang, L., Wang, X., Jing, A., Zhao, B., Yu, X., Zheng, J., and Zhou, F. (2015) Tabersonine inhibits amyloid fibril formation and cytotoxicity of Aβ(1−42). *ACS Chem. Neurosci. 6*, 879−888.
(56) Barr, R. K., Verdile, G., Wijaya, L. K., Morici, M., Taddei, K., Gupta, V. B., Pedrini, S., Jin, L., Nicolazzo, J. A., Knock, E., Fraser, P. E., and Martins, R. N. (2016) Validation and characterization of a novel peptide that binds monomeric and aggregated β-amyloid and inhibits the formation of neurotoxic oligomers. *J. Biol. Chem. 291*, 547−559.

DOI: 10.1021/acschemneuro.6b00154
ACS Chem. Neurosci. XXXX, XXX, XXX−XXX